

Title	Initial Fatigue Crack Growth Behavior in a Notched Component (Report III) : Effect of Cyclic Yield Strength(Mechanics, Strength & Structural Design)
Author(s)	Horikawa, Kohsuke; Cho, Sang-moung
Citation	Transactions of JWRI. 1987, 16(2), p. 367-373
Version Type	VoR
URL	https://doi.org/10.18910/8831
rights	
Note	

Osaka University Knowledge Archive : OUKA

<https://ir.library.osaka-u.ac.jp/>

Osaka University

Initial Fatigue Crack Growth Behavior in a Notched Component (Report III)[†]

—Effect of Cyclic Yield Strength—

Kohsuke HORIKAWA* and Sang-moung CHO**

Abstract

The present report was intended to evaluate the difference of initial fatigue crack propagation rate between mild steel and high tensile strength steel in notch field subjected to high stress.

The two used materials (SS41, HT80) had similar characteristics in long crack propagation ($R = -1$) when small scale yield condition was satisfied. However in low cycle (high stress) region ($R = -1$), initial fatigue crack propagation rate in center notched strip of SS41 was higher than that of HT80. This characteristics might result from elasto-plastic effect on fatigue crack propagation. By application of ΔJ calculated in this study, the elasto-plastic effect could be evaluated.

As the results, it would be mentioned that initial fatigue crack propagation rate in notch field taking elasto-plastic behavior can be estimated from master curve of long crack by using ΔJ in which cyclic yield strength of material is considered.

KEY WORD: (Fatigue Crack Propagation) (Notch Field) (Initial Fatigue Crack) (Elasto-Plastic Effect) (Cyclic Yield Strength) (ΔJ)

1. Introduction

In the case of considering fatigue crack initiation life in structural discontinuity (Notch) which is free from defect, the difference of fatigue strength between mild steel and high tensile strength steel in low cycle region of S-N curve can be interpreted by local mechanical quantity and cyclic material constants¹⁻⁴.

However, the difference of initial crack propagation rate between mild steel and high tensile strength steel in notch field subjected to high stress may have not been clarified till now with fracture mechanics.

When fatigue crack propagation life is evaluated by ΔK based on LEFM, elasto-plastic effect of materials due to high stress is not considered, because the behavior of material is assumed to be linear elastic.

Therefore, in the previous report⁵, crack extension force ΔJ in notch field was evaluated by considering elasto-plastic effect and crack closure behavior. The applicability of the ΔJ was confirmed by fatigue tests ($R = -1$) to center notched strips.

The present report is intended to evaluate the difference of initial fatigue crack propagation rate between mild steel (SS41) and high tensile strength steel (HT80) in notch

field subjected to high stress. These two steels (SS41, HT80) were tested to investigate long crack propagation characteristics when small scale yield condition was satisfied. Initial crack propagation tests to two kinds of notched strips made of the steels were performed. And the effect of cyclic yield strength on initial crack propagation rate was examined.

2. Specimens and Experimental Procedure

The materials used in experiments were mild steel (SS41) and high tensile strength steel (HT80). 4 kinds of specimens shown in Fig. 1 were tested. Smooth specimen of Fig. 1 (a) was used to investigate cyclic stress-strain relation obtained by the companion specimens method, in which axial strain was controlled ($R_\epsilon = -1$). Center cracked specimen of Fig. 1 (b) was tested to investigate long crack propagation characteristic which was used as the master curve of the material. Center notched specimens (2B = 36mm) of Fig. 1 (c) was tested to observe initial crack propagation behavior in notch field. As shown in Fig. 1 (c), the notch root radius ρ of elliptical hole was 0.25mm ($Kt = 6.0$), circular hole was 2.5mm ($Kt = 2.7$).

Transactions of JWRI is published by Welding Research Institute of Osaka University, Ibaraki, Osaka 567, Japan

[†] Received on Nov. 4, 1987

* Professor

** Graduate Student

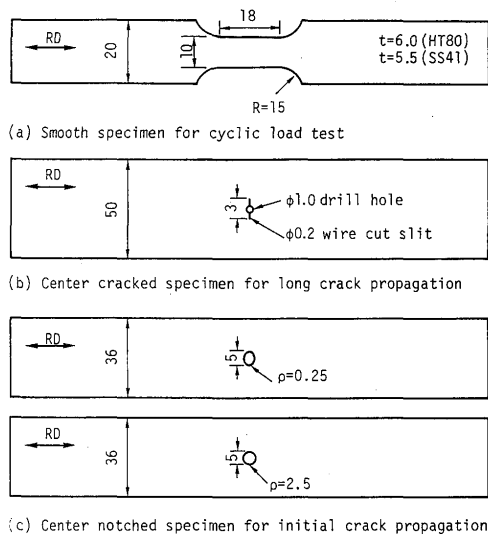


Fig. 1 Configuration of specimens.

All notches were processed by electrodischarge.

All crack propagation tests for center cracked and notched specimens of Fig. 1 (b) (c) were carried out under constant amplitude of fully reversed axial load control ($R = -1$). Load speed of sine wave was 0.5 ~ 10 Hz. Crack length was measured on both surface of front and back by travelling microscope (X50). All tests were performed at ambient room temperature.

3. Experimental Results and Discussion

3.1 Cyclic stress-strain relation of the materials

Fig. 2 indicates the relation of stress and strain amplitude at the half of failure life in the companion specimens method for smooth specimens of Fig. 1 (a). The dot-and-dash lines in Fig. 2 mean monotonic stress-strain curves by tensile tests.

HT80 steel showed cyclic softening property. SS41 steel was softened in the region of low strain amplitude (about 0.2%), but hardened in the region of high strain amplitude. As a general trend on the two cyclic stress-strain curves, HT80 showed considerably higher strength than SS41.

As the relation of stress amplitude σ_a and strain amplitude ϵ_a , which is used to calculate ΔJ , piecewise power hardening rule was used as follows.

$$\sigma_a = E\epsilon_a, \quad \sigma_a \leq \sigma_{YC} \dots \dots \dots (1.1)$$

$$(\sigma_a/\sigma_{YC}) = (\epsilon_a/\epsilon_{YC})^{n'}, \quad \sigma_a > \sigma_{YC} \dots \dots \dots (1.2)$$

where, $\epsilon_{YC} = \sigma_{YC}/E$

The results of cyclic load tests were applied to Eq. (1), and then the solid lines in Fig. 2 were used as the cyclic stress-strain curves of two materials. And in Table 1 material constants for the solid lines are given.

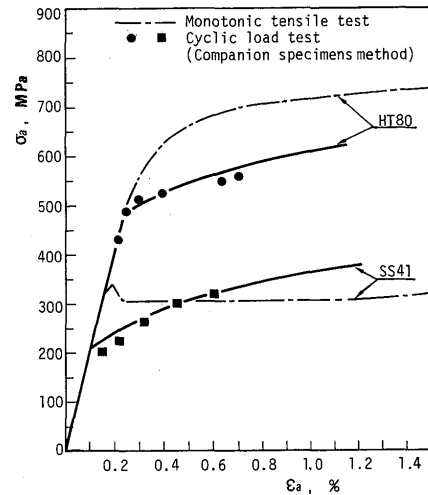


Fig. 2 Relation of cyclic stress-strain in HT80

Table 1 Material constants in cyclic stress-strain curve

Material	E(GPa)	σ_{YC} (MPa)	n'
HT80	205.8	480.0	0.167
SS41	205.8	205.0	0.25

3.2 Long crack propagation properties for materials

In this section, when small scale yield condition was satisfied in center cracked specimen of Fig. 1 (b), long crack propagation rate was evaluated. Load condition was limited so that the small scale yield condition could be satisfied as follows⁶⁾.

$$0.8\sigma_{YS} \geq P_{max}/(A)_{liga} \dots \dots \dots (2)$$

where, σ_{YS} indicates monotonic yield strength by 0.2% off-set.

HT80: $\sigma_{YS} = 676$ MPa

SS41: $\sigma_{YS} = 305$ MPa

P_{max} : Maximum tensile load

$(A)_{liga}$: Sectional area of uncracked ligament

Crack propagation rate was evaluated after a crack was grown over 1.5mm from the slit tip.

Fig. 3 shows the characteristics of long crack propagation rate for SS41 and HT80. ΔK was calculated from $K_{max}-K_{min}$, the effect of crack closure was disregarded. In the region of low ΔK , crack propagation rate of SS41 was lower than that of HT80. However it was regarded

that the crack propagation rates in the linear parts of the two curves were almost the same. This is similar to the general tendency that appears when mechanical properties such as yield strength are different in various structural steels^{7,8)}.

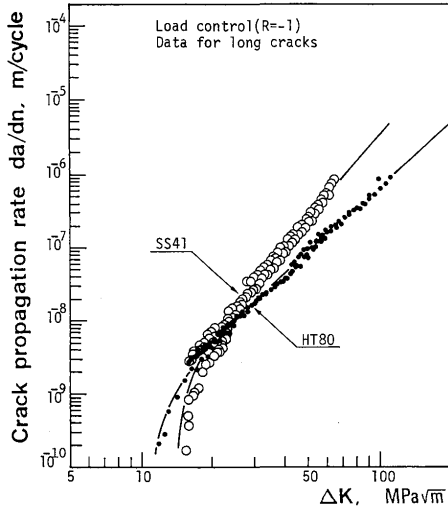


Fig. 3 Relation of ΔK - da/dn for long cracks.

In Fig. 4, the characteristics of long crack propagation rates were evaluated in consideration of crack opening ratio U for two materials. ΔJ could be obtained from $\Delta J = \Delta K_{eff}^2/E = (U \Delta K)^2/E$ when plane stress state was presumed. The crack opening ratio U was obtained by the following empirical formular, which was derived by some modification and simplification of the empirical formulars in the previous report ($R = -1$)⁵⁾.

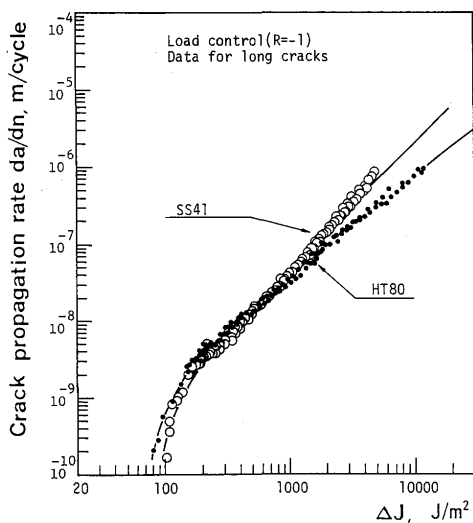


Fig. 4 Relation of ΔJ - da/dn for long cracks considering crack opening ratio.

$$U = U_e + (1 - U_e) \tanh \{0.71 \log (\epsilon_{max}/\epsilon_{YC} + 0.6)\} \dots \dots \dots (3)$$

Where, ϵ_{max} is nominal strain at the maximum tensile load. U_e is crack opening ratio at $\epsilon_{max}/\epsilon_{YC} = 0.4$ in elastic state. U_e for HT80 was 0.42 ($R = -1$), and for SS41 was 0.4 ($R = -1$).

In Fig. 4, it is recognized that the difference of long crack propagation characteristics for two steels are decreased by adopting ΔJ rather than ΔK . Namely, even though monotonic and cyclic yield strength of two steels are different, it can be confirmed that the characteristics of long crack propagation, when small scale yield condition is satisfied, are nearly the same.

3.3 ΔK - da/dn relation in notch field

The small scale yield condition is not satisfied in the case of initial fatigue crack in notch field which behaves elasto-plastically. This initial fatigue crack propagation rate was evaluated by ΔK so that the effect of cyclic yield strength on initial crack propagation is manifested. In this case, ΔK was calculated from the following formula using nominal stress range $\Delta\sigma$ ^{5), 9), 10)}.

$$\Delta K = \Delta\sigma \sqrt{\pi(a + a_0)} F(a) \dots \dots \dots (4)$$

where, a is crack length from notch tip

a_0 is notch length

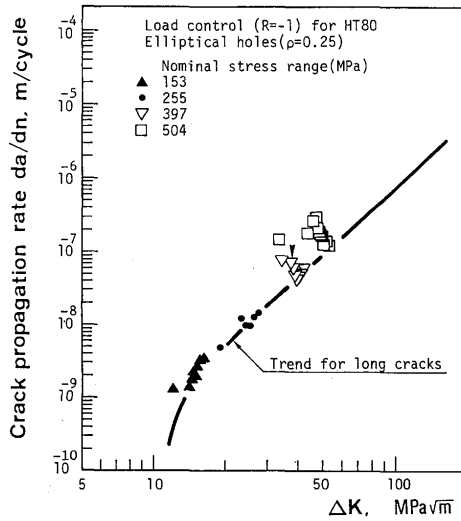
$F(a)$ is the geometric correction factor

Material constants are not involved in Eq. (4), and the ΔK is governed by nominal stress which is linearly proportional to external load, and governed by the geometry.

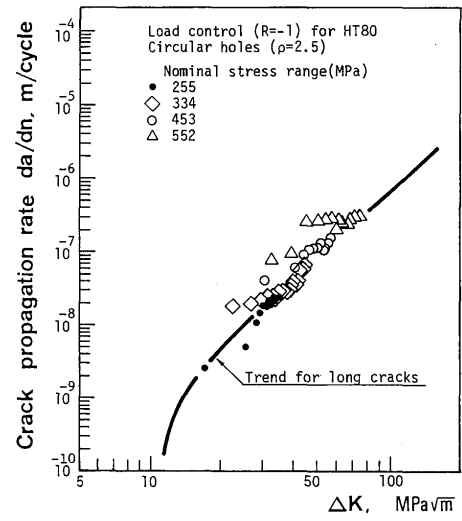
Fig. 5 (a) (b) show the relation of ΔK - da/dn in notch field of elliptical hole ($\rho = 0.25$) for HT80 and SS41. Each solid line is master curve which is obtained from the characteristic of long crack propagation on each material in Fig. 3. And initial crack propagation rate in notch field was evaluated till crack length a from notch tip becomes $\sqrt{a_0\rho}$, because the notch field had been defined as the range from notch tip to $\sqrt{a_0\rho}$ in the first report¹¹⁾.

From Fig. 5, it can be mentioned that the extent to deviate from master curve is more remarkable in SS41 than in HT80.

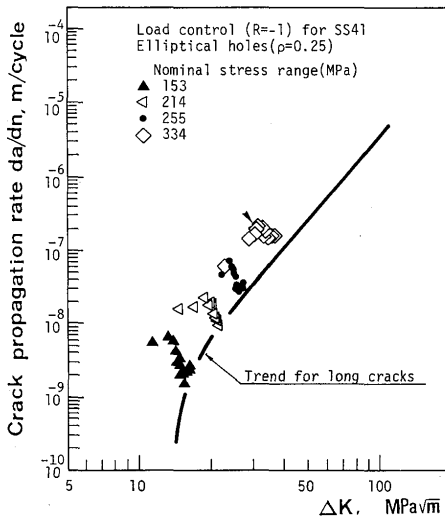
Fig. 6 (a) (b) indicate the relation of ΔK - da/dn in notch field of circular hole ($\rho = 2.5$) for HT80 and SS41. Also in Fig. 6, the extent to deviate from master curve is more distinguished in SS41 than in HT80. From this tendency, it can be examined that the effect of elasto-plastic behavior on initial crack propagation in notch field is greater in SS41 which have lower cyclic yield strength than in HT80 which have higher that. Moreover, in Fig. 5



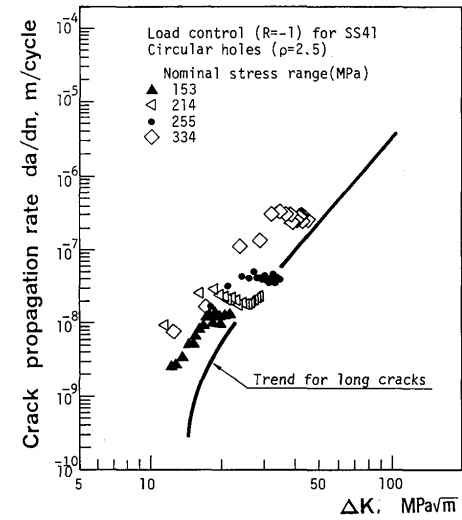
(a) HT80(ρ=0.25)



(a) HT80 (ρ=2.5)



(b) SS41(ρ=0.25)



(b) SS41 (ρ=2.5)

Fig. 5 Relation of ΔK - da/dn for initial cracks in notch field ($\rho = 0.25$)

Fig. 6 Relation of ΔK - da/dn for initial cracks in notch field ($\rho = 2.5$)

and Fig. 6, the lower nominal stress level is, and the longer crack length from notch tip is, the closer the characteristic of initial crack propagation is to the trend of master curve. This tendency means that elasto-plastic effect depends on stress distribution in notch field when crack is not existent. The stress distribution is the function of nominal stress level, notch shape and material constants (mainly cyclic yield strength). Therefore, it can be said that elasto-plastic effect on initial crack propagation is controlled by above three factors.

Especially, in the two materials which have nearly same characteristics of long crack propagation, even though notch shape and nominal stress level are the same, elasto-plastic effect in SS41 is more conspicuous than in HT80. This may result from that cyclic yield strength of SS41 is

lower than that of HT80.

In consequence, the effect of cyclic yield strength on initial crack propagation rate in notch field could be confirmed directly.

3.4 ΔJ - da/dn relation in notch field

In this section, ΔJ was used for correlating initial crack propagation rates in notch field.

Crack opening ratio U to consider elasto-plastic behaviour of notch field was used for calculating ΔJ . It may be reasonable to use the measured U for calculating ΔJ . But it may be difficult to measure the U for engineering structures. Therefore, the empirical formula Eq. (3) can be used for estimating the U . To apply Eq. (3) for

notch field, equivalent strain $\bar{\epsilon}_{\max}(\mathbf{a})$ at crack tip corresponding point in maximum load when crack is not existent, was substituted for ϵ_{\max} to be maximum nominal strain.

If crack opening ratio U is obtained as the function of crack length in notch field, then $\Delta\bar{\sigma}_{\text{eff}}(\mathbf{a}) = U\Delta\bar{\sigma}(\mathbf{a})$ can be estimated. When plane stress is assumed, and $\phi_a = \Delta\bar{\sigma}(\mathbf{a})/2\sigma_{YC}$ is given, ΔJ can be calculated as follows⁵⁾.

$$\Delta J = \Delta J_e = \Delta K_{\text{eff}}^2/E = \{C_N \Delta\bar{\sigma}_{\text{eff}}(\mathbf{a}) \sqrt{\pi a}\}^2/E,$$

$$\phi_a \leq 1.0 \dots \dots \dots (5.1)$$

$$\frac{\Delta J}{\Delta J_e} = 1.0 + \frac{1}{C_N^2 \pi} \{ \phi_a^{(1+n')/n'} - 1 \} \frac{h(n')C_p}{\phi_a^2},$$

$$\phi_a > 1.0 \dots \dots \dots (5.2)$$

where, C_N is the geometric correction factor based on equivalent stress in notch field.

$h(n')$ is the function of He and Hutchinson¹²⁾, and controlled by material, stress state and geometry. In the case of small edge crack in semi-infinite plate, $h(n') = 10.04$ (HT80), $h(n') = 8.12$ (SS41).

C_p is the plastic constraint coefficient and given by⁵⁾,

$$C_p = \tanh \left\{ \frac{1}{4} \sqrt{\frac{\rho}{2.32n'}} \right\} \dots \dots \dots (6)$$

Fig. 7 (a) (b) show the relation of ΔJ - da/dn in notch field of elliptical hole ($\rho = 0.25$). Fig. 8 (a) (b) are that of circular hole ($\rho = 2.5$). Each solid line is master curve obtained from long crack propagation (ΔJ - da/dn) for each

material as shown in Fig. 4.

From Fig. 7 and Fig. 8, it can be found out that the deviation from master curve is very small regardless of nominal stress level, geometry and material. Namely, fatigue crack propagation rate from initial to long crack can be evaluated by ΔJ regardless of the satisfaction of small scale yield condition and of cyclic yield strength level. Because the parameters on elasto-plastic effect and cyclic yield strength are taken into account in calculating ΔJ as shown in Eq. (5).

As a result, initial crack propagation rate in elasto-plastic notch field is able to predict by using master curve if ΔJ is determined.

3.5 Discussion

Fig. 9 shows the appearance of strain gages to observe elasto-plastic behavior of notch field having a crack. Load direction is y-direction, and then ϵ_x measured by strain gages in Fig. 9 is perpendicular to load direction.

In Fig. 10 (a) (b), elasto-plastic behavior of notch field ($\rho = 0.25$) having fatigue crack is compared for the two materials. Fig. 10 (a) is $P - \epsilon_x$ diagram obtained from the state that nominal stress range $\Delta\sigma = 397$ MPa was loaded to HT80. Fig. 10 (b) is also $P - \epsilon_x$ diagram when $\Delta\sigma = 334$ MPa was loaded to SS41. Nominal stress range was lower in SS41 than in HT80. However, in the case of crack length $a = 0.26$ mm in SS41, remarkable elasto-plastic behavior can be recognized from the large hysteresis loop. But, when crack length a is 1.93 mm in SS41, elasto-plastic behavior is very decreased.

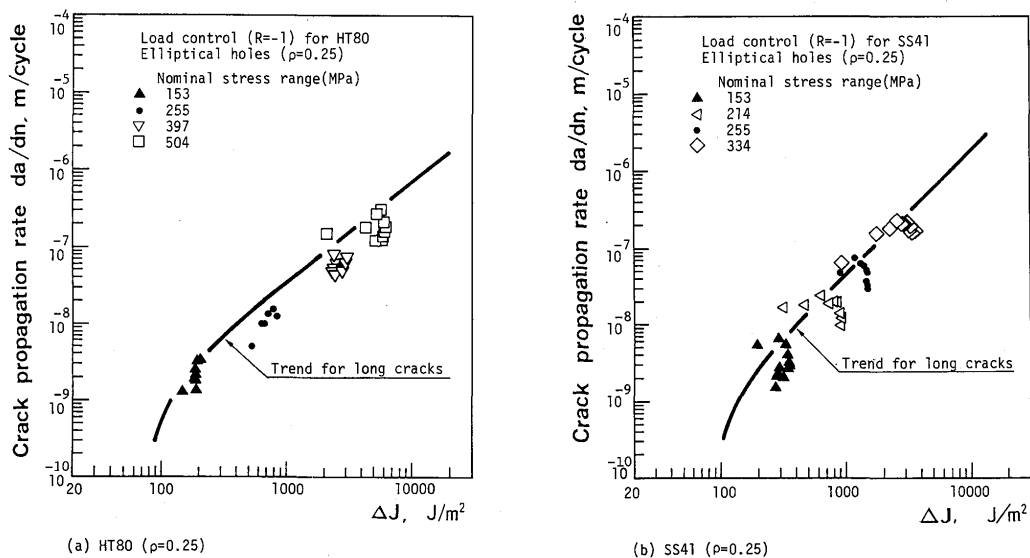


Fig. 7 Relation of ΔJ - da/dn for initial cracks in notch field ($\rho = 0.25$)

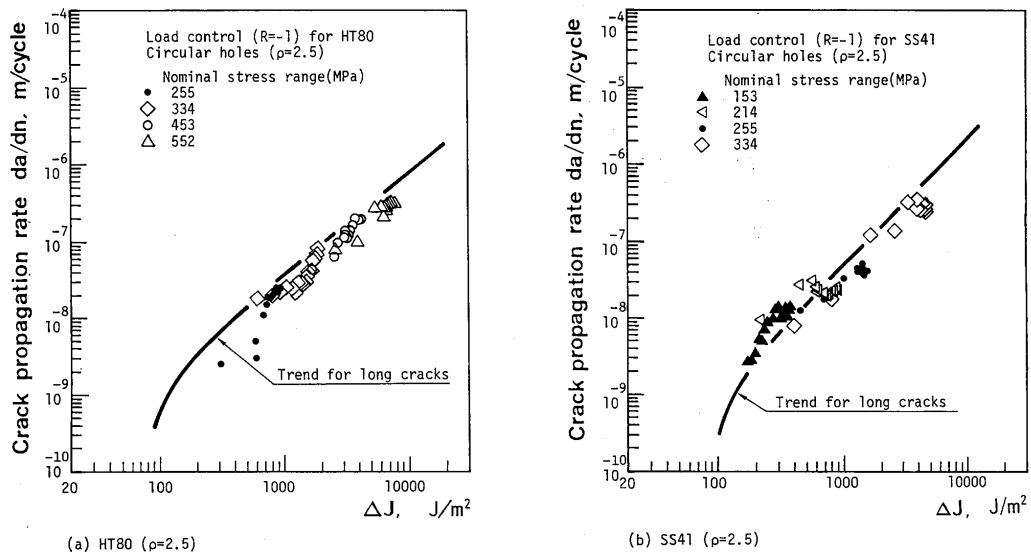


Fig. 8 Relation of ΔJ - da/dn for initial cracks in notch field ($\rho = 2.5$).

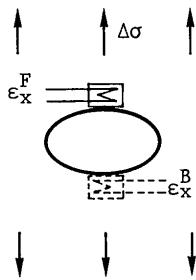


Fig. 9 Location of strain gages to obtain $P - \epsilon_x$ hysteresis loops

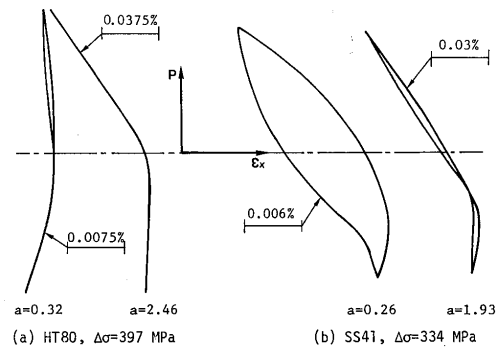


Fig. 10 Comparison of elasto-plastic behavior between HT80 and SS41 in notch field with fatigue cracks ($\rho = 0.25$)

By the way, for each crack length in Fig. 10 (a) (b), $\phi_a = \Delta \bar{\sigma}(a) / 2 \sigma_{YC}$ was calculated, and indicated in Table 2. The stress range $\Delta \bar{\sigma}(a)$ was, as aforesaid, equivalent stress range at the crack tip corresponding point when crack was not existent. When a crack was grown over notch field ($= \sqrt{a_0 \rho}$), $\Delta \bar{\sigma}(a)$ was determined from $\Delta P / A_{net}$ (A_{net} : net sectional area when crack was not existent). Considering Fig. 10 (a) (b) and ϕ_a in Table 2, in the case that ϕ_a is higher than 1.0, loading and unloading path is different, and hysteresis loop is depicted. From Fig. 10 (a) (b), each crack propagation rate for $a = 0.32$ mm (HT80) and $a = 0.26$ mm (SS41) in notch field was indicated by attaching an arrow on $\Delta K - da/dn$ relation in Fig. 5 (a) (b). It can be regarded that the extent to deviate from master curve depend upon the level of ϕ_a .

From the above discussion on elasto-plastic behavior of notch field having a crack, the two followings are able to be mentioned.

(1) If notch field having initial crack takes elasto-plastic

Table 2 Normalized local stress level at crack tip corresponding point ($\rho = 0.25$)

	HT80		SS41	
a	0.32	2.46	0.26	1.93
ϕ_a	1.03	0.48	1.54	0.95

$$\phi_a = \Delta \bar{\sigma}(a) / 2 \sigma_{YC}$$

behavior, and then elasto-plastic effect appears in crack propagation.

(2) The aforesaid three factors governing the elasto-plastic effect, namely nominal stress level, geometry and material constants, can be evaluated inclusively by $\phi_a = \Delta \bar{\sigma}(a) / 2 \sigma_{YC}$.

Fig. 11 (a) (b) show the relation of da/dn and crack length, and of ΔJ and crack length in circular notch field ($\rho = 2.5$) of the two materials. Nominal stress range $\Delta \sigma$ was 255.0 MPa in all cases of Fig. 11. When crack is not initiated, the notch tip of HT80 takes elastic behavior, but

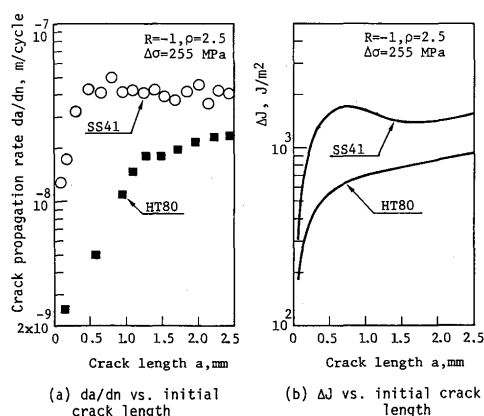


Fig. 11 Comparison of da/dn and ΔJ between HT80 and SS41 in notch field ($\rho = 2.5$)

in notch field of SS41 cyclic plastic zone is developed because cyclic yield strength of it is lower than HT80. Moreover, initial crack in HT80 grows into elastic zone, but in SS41 does into cyclic plastic zone formed previously by stress concentration of notch. In consequence, as shown in Fig. 11 (a) initial crack in SS41 propagates with higher rate than in HT80. Fig. 11 (b) indicates variation of ΔJ in notch field in the same case. This trend on ΔJ corresponds well with that on da/dn of Fig. 11 (a). And as crack length becomes long, da/dn and ΔJ in SS41 close to those in HT80. This trend result from that as a crack grows into elastic zone after it passes through plastic zone of notch in SS41, and crack propagation turns into to be not contributed by elasto-plastic effect.

4. Conclusions

In notch field taking elasto-plastic behavior, the effect of cyclic yield strength on initial crack propagation was examined. The used materials were HT80 and SS41. Fully reversed ($R = -1$) fatigue tests were carried out.

The main results are as follows.

- (1) When small scale yield condition was satisfied, the characteristics of long crack propagation in SS41 and HT80 became nearly the same in spite of different monotonic and cyclic yield strength. (Fig. 3 and Fig. 4)
- (2) When initial crack propagation rate was evaluated by ΔK , deviation from the master curve was more remarkable in SS41 than in HT80 although the same nominal stress and notch geometry. This means that

elasto-plastic effect contributes more to SS41 than HT80 because cyclic yield strength of the former was lower than the latter. In consequence, the effect of only cyclic yield strength on initial crack propagation could be confirmed in notch field. (Fig. 5 and Fig. 6)

- (3) By using ΔJ to take cyclic yield strength into consideration, the initial crack propagation property coincided well with the master curve. (Fig. 7 and Fig. 8)
- (4) Elasto-plastic effect on initial crack propagation in notch field could be evaluated very inclusively by $\phi_a = \Delta \bar{\sigma} (a) / 2 \sigma_{YC}$. (Fig. 10 and Table 2)

Reference

- 1) M. Nihei, P. Heuler, C. Boller, T. Seeger: Fatigue Life Prediction by Use of Damage Parameters, Tran. S. Naval Architects of Japan, 156 (1984), pp469-477 (in Japanese).
- 2) D.F. Socie: Fatigue-life Prediction Using Local Stress-Strain Concepts, Expt. Mech. (Feb. 1977), pp50-56.
- 3) T.R. Gurney: Fatigue of Welded Structures, Cambridge Univ. Press, (1979), pp196-211.
- 4) K. Iida: Application of the Hot Spot Strain Concept to Fatigue Life Prediction, Doc. IIS/IIW-780-83, Welding in the World 22-9/10 (1984), pp222-246.
- 5) K. Horikawa, S.-M. Cho: Initial Fatigue Crack Growth Behavior in a Notched Component (Report II), Tran. JWRI. 16-1 (1987), pp167-175.
- 6) ASTM E647-83: Constant-Load-Amplitude Fatigue Crack Growth Rate above 10^{-8} m/cycle, ASTM Designation, pp710-730.
- 7) A. Ohta, E. Sasaki: Fatigue Crack Propagation Properties in Arc-welded Butt-joints of High Strength Steels for Welded Structure, National Research Institute for Metals, Fatigue Data Sheet 3. (in Japanese).
- 8) K. Yamada: Fatigue Crack Growth Rates of Structural Steels under Constant and Variable Amplitude Block Loading, Proc. of JSCE, Structural Eng./Earth-quake Eng., 2-2 (1985), pp271s-279s.
- 9) M. Isida: Elastic Analysis of Cracks and Stress Intensity Factor, Baihukan, Tokyo, Japan (1981), pp170-174 (in Japanese).
- 10) Y. Nakai, S. Kubo, K. Ohji: Approximation Formula on Stress Intensity Factor of Crack initiated in Notch Field, Tran. Japan Society of Mechanical Engineers (A), 50-460 (1984), pp2017-2021 (in Japanese).
- 11) K. Horikawa, S.-M. Cho: Initial Fatigue Crack Growth Behavior in a Notched Component (Report I), Tran. JWRI. 16-1 (1987), pp159-166.
- 12) M.Y. He, J.W. Hutchinson: Bounds for Fully Plastic Crack Problems for Infinite Bodies, ASTM STP 803 (1983), pp1277-1290.